Supplement of Atmos. Chem. Phys., 23, 8241–8257, 2023
https://doi.org/10.5194/acp-23-8241-2023-supplement

Atmospheric Chemistry and Physics
Open Access

Supplement of

Characterization of dust-related new particle formation events based on long-term measurement in the North China Plain

Xiaojing Shen et al.

Correspondence to: Xiaojing Shen (shenxj@cma.gov.cn)

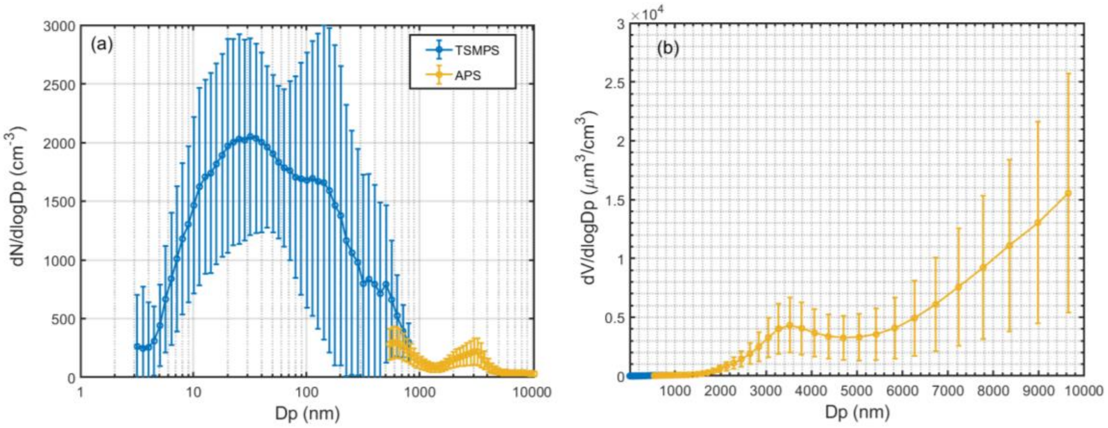

Fig. S1 The number size distribution (a) and volume size distribution (b) derived from TSMPS and APS.

The potential source contribution function (PSCF) analysis method has been widely applied to study the potential source regions of pollutants (Ashbaugh et al., 1985; Wang, et al., 2009). The PSCF values for each grid cell (0.5°*0.5°) in the selected domain were calculated by counting the number of trajectories those terminated within each grid cell, as follows:

$$PSCF_{ij} = \frac{m_{ij}}{n_{ij}} \quad (1)$$

where n_{ij} is the number of endpoints that fall in the ijth cell, and m_{ij} is the number of endpoints for the same cell with pollutant concentrations higher than the set criterion value. The PSCF values should be weighted according to n_{ij}. In this study, the weighting function (W_{ij}) was defined as follows:

$$W_{ij} = \begin{cases} 1.00 & 10 \times \overline{n_{ij}} < n_{ij} \\ 0.70 & 5 \times \overline{n_{ij}} < n_{ij} \leq 10 \times \overline{n_{ij}} \\ 0.40 & 2 \times \overline{n_{ij}} < n_{ij} \leq 5 \times \overline{n_{ij}} \\ 0.05 & n_{ij} \leq 2 \times \overline{n_{ij}} \end{cases} \quad (2)$$

where $\overline{n_{ij}}$ is the mean n_{ij} value. In this study, a potential source analysis was conducted for the nucleation and accumulation mode particles, which represented the air mass influence on the NPF event and the particles from long-range transport, respectively. The criterion values of $PM_{2.5}$ and PM_{10} mass concentration were 75 μg cm^{-3} and 100 μg cm^{-3}, which was the mean value in March, April and May in 2021.

The PSCF results (Fig. S1) showed that high $PM_{2.5}$ mass concentration at CAMS was dominated by two sources, the northwesterly and westerly originating air mass containing dust particles, and the southerly air mass with high mass loading of anthropogenic aerosols. However, for PM_{10} mass concentration, the high values only contributed by the air masses passing through Inner Mongolia and carrying dust particles.

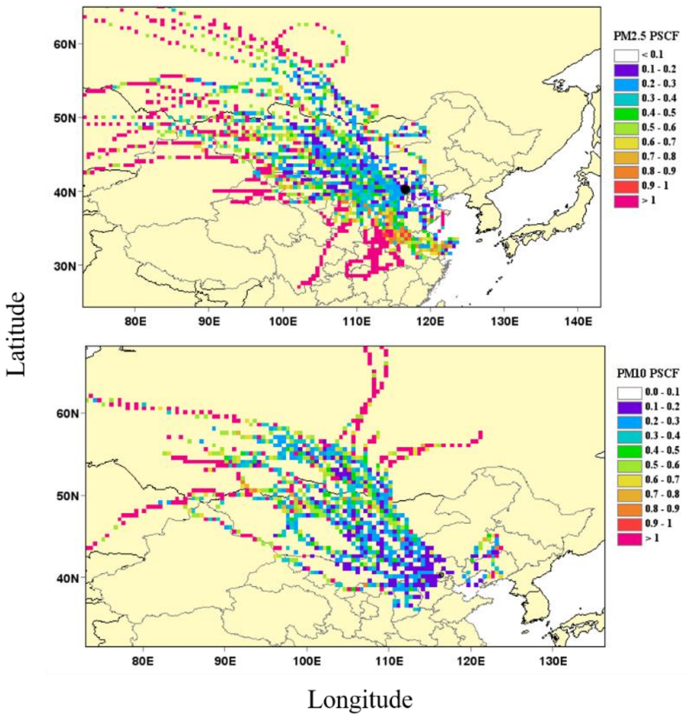

Fig. S2. Air mass classification of back trajectories arriving at the CAMS site in March, April and May, 2021. The color bar indicates the number concentration weighted potential source contribution function (PSCF) value of (upper panel) $PM_{2.5}$ and (lower panel) PM_{10} mass concentration.

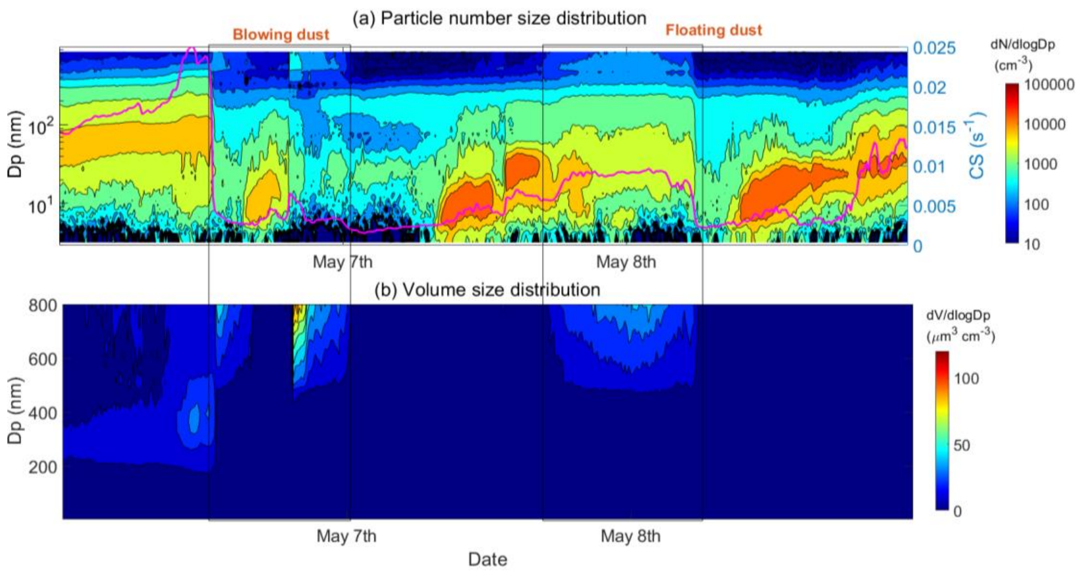

Fig. S3 NPF event occurred following blowing dust (May 6 and 7) and floating dust (May 8) in 2021. The particle number (a) and volume (b) size distribution are given and *CS* is given by pink line.

The reactive gases (SO_2, NO_2, and O_3) were derived as the average of the values at four air quality monitoring sites, including Guanyuan (GY), Wanshou Temple (WST), Dongsi (DS), and Chaoyang (CY), in urban Beijing, as mentioned in the manuscript. It showed before NPF start, around 8:00 LT, the concentration of SO_2 and NO_2 on May 7 and 8 was quite close, which did not show a clear difference between workday and weekend. Furthermore, the *CS* before NPF start was also comparable on these two days, around 0.003 s^{-1}, indicating the available condensable vapor was close.

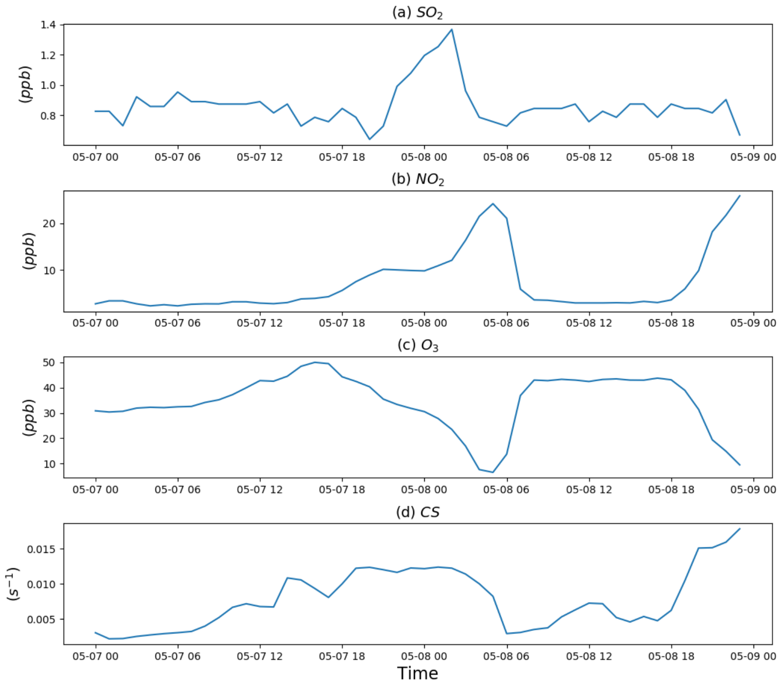

Fig. S4. Time series of hourly volume mixing ratio of SO_2, NO_2, O_3 and condensation sink (*CS*) on May 7 and 8, 2021.

As there is no direct H_2SO_4 measurement data available in this work, we used two methods to estimate sulfuric acid concentration. In the calculation of [H_2SO_4] in Beijing, we chose proxy equation number 2 as Proxy 1 in this study (Eq. 1) and 7 (Eq. 2) as Proxy 2 in this study as recommended by Lu et al. (2019), to represent the simplest and most accurate method, respectively.

$$[H_2SO_4] = 280.05 \times UVB^{0.14} \times [SO_2]^{0.40} \quad (1)$$

$$[H_2SO_4] = 0.0013 \times UVB^{0.13} \times [SO_2]^{0.40} \times CS^{-0.17} \times ([O_3]^{0.44} + [NO_x]^{0.41}) \quad (2)$$

And the UVB was derived by 0.008% × Glob_R, based on the previous study that the monthly average of the ratio of UVB to global radiation (Glob_R) ranged from 0.007 to 0.017% in Beijing (Hu et al., 2013). The average ratio of January and February (0.008%) was applied.

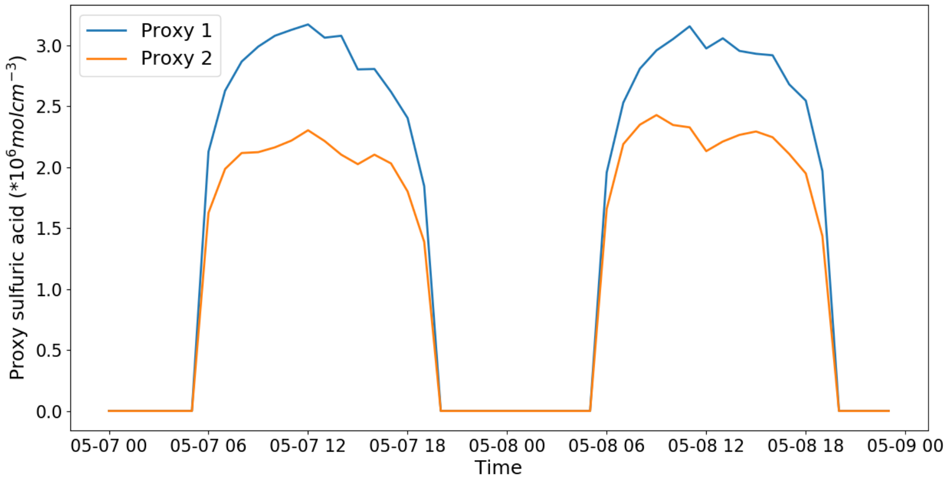

Fig. S5. The sulfuric acid concentrations derived by different proxy equations. The blue and orange lines indicate the result by N2 (Proxy 1) and N7 (Proxy 2) method by Lu et al., (2019).

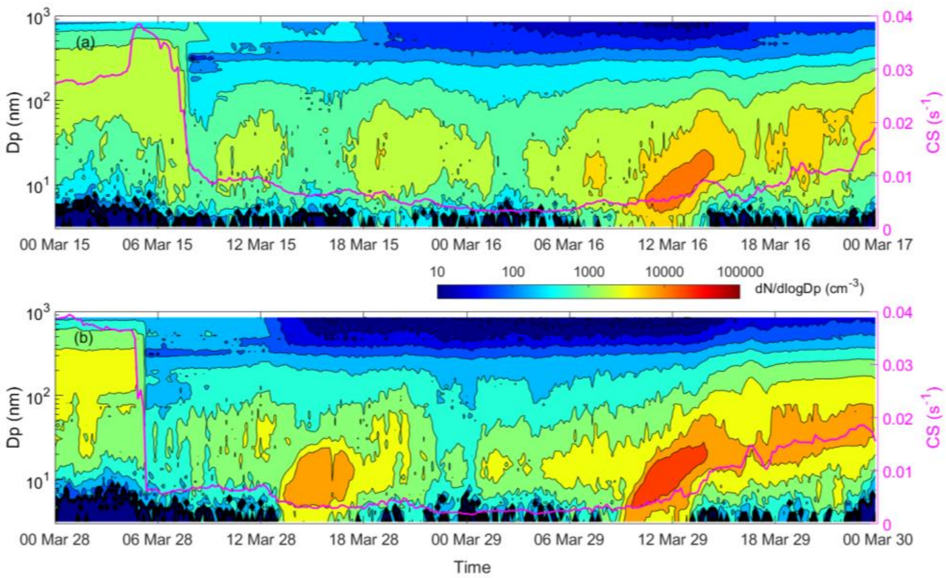

Fig. S6 The NPF event occurred after dust storm on March 15 (a) and blowing dust on March 28, 2021 (b), respectively. The pink line in panel indicates the condensation sink.

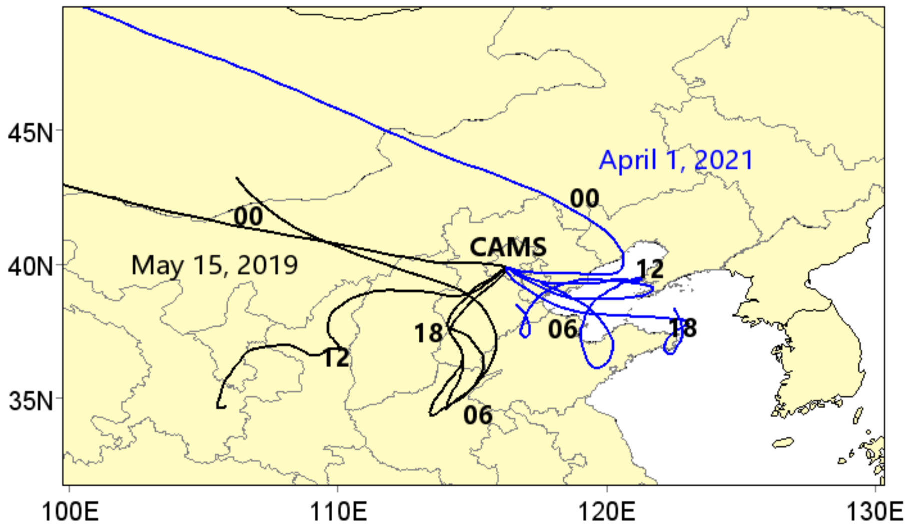

Fig. S7 The 72 hours back trajectories arriving at CAMS station at four times a day (00, 06, 12, 18 UTC) on May 15th 2019 (black lines) and April 1st 2021 (blue lines) with the terminal height of 500 m above ground level, derived by the TrajStat software, combined with HYSPLIT 4 model

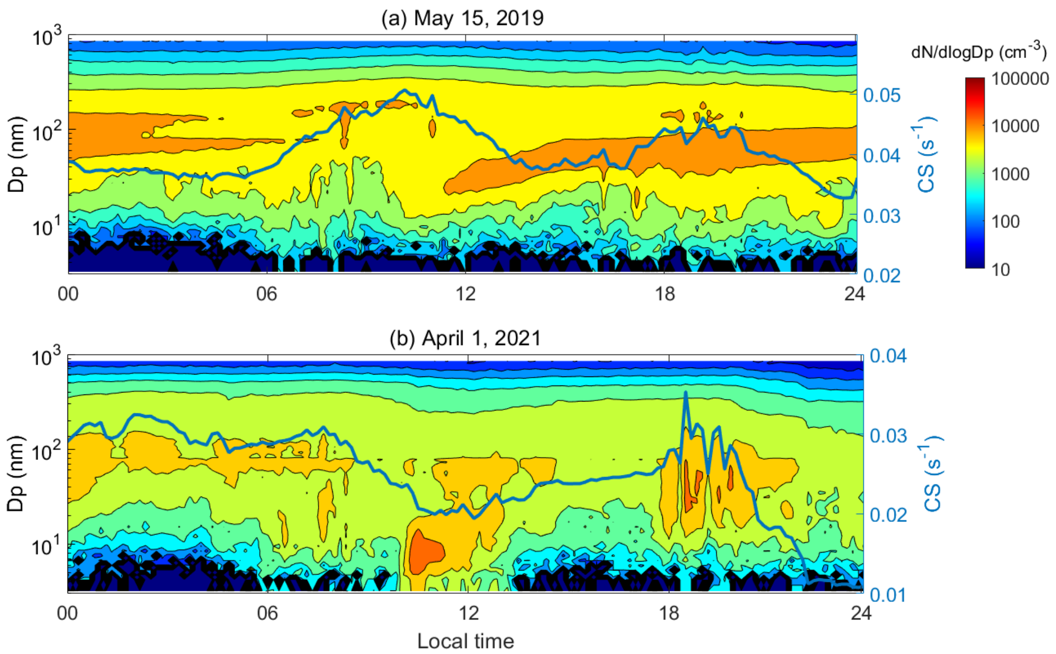

Fig. S8 PNSD of NPF events on May 15th 2019 and April 1st 2021, the condensation sink (*CS*) was given in blue line.

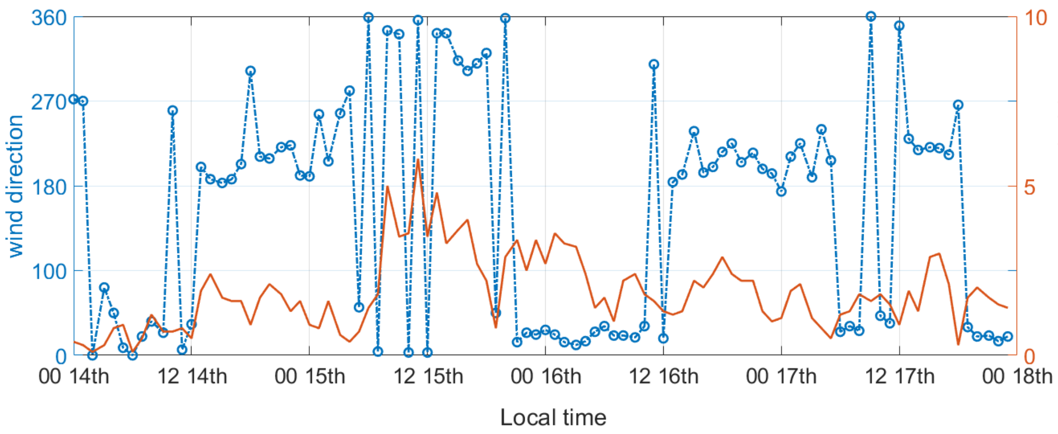

Fig. S9 The wind direction and wind speed at CAMS site from March 14th to 17th.

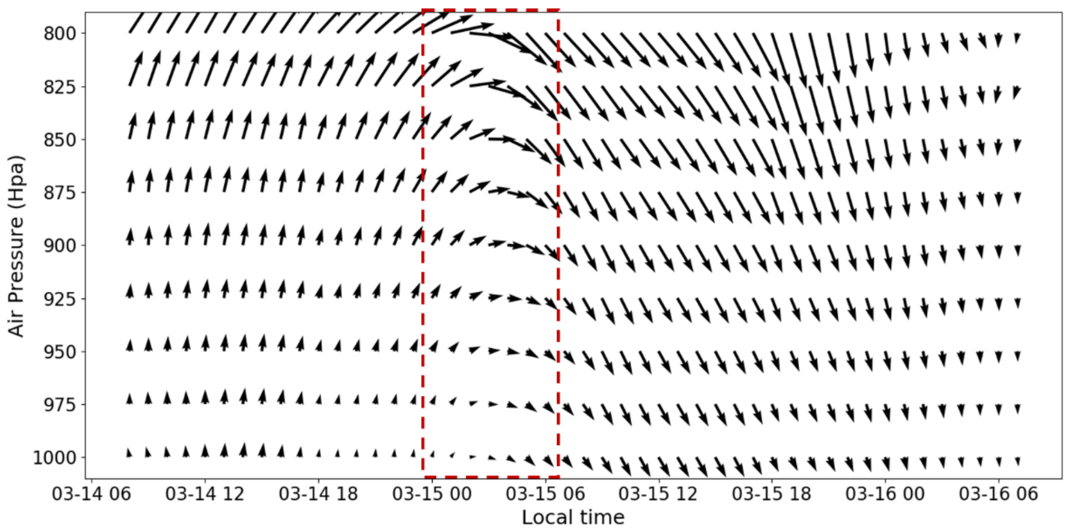

Fig. S10. Time series of wind variation depending on the air pressure level from March 14 to 15, the arrows represent the wind direction and the length of the arrow indicates the wind speed (m/s). The data are from https://cds.climate.copernicus.eu/.

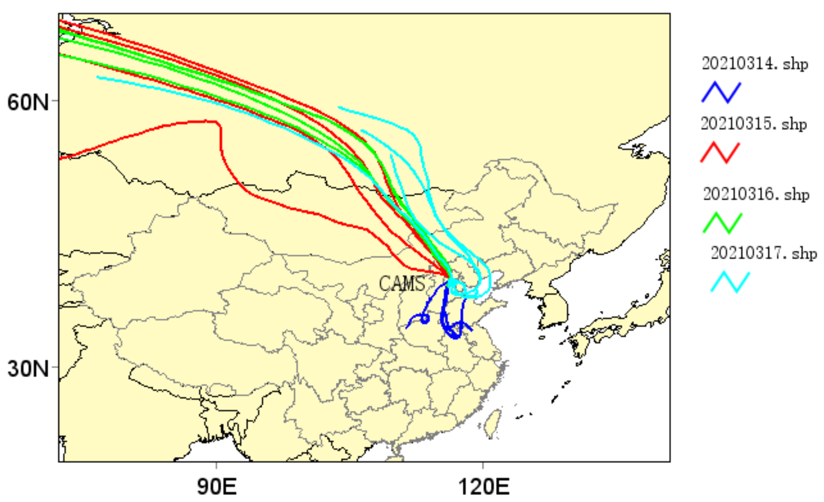

Fig. S11 The 72 hours back trajectories arriving at CAMS station at four times a day

(00, 06, 12, 18 UTC) from March 14th to 17th with the terminal height of 500 m above ground level, derived by the TrajStat software, combined with HYSPLIT 4 model (Hybrid Single-Particle Lagrangian Integrated Trajectory), and the NCEP Global Data Assimilation System (GDAS) data with a 1° × 1° resolution (Draxler and Hess, 1998; Wang et al., 2009)

Reference:

Ashbaugh, L.L., Malm, W.C., Sadeh, W.Z., 1985. A residence time probability analysis of sulfur concentrations at Grand Canyon National Park. Atmospheric Environment 19 (8), 1263–1270.

Draxler, R.R., Hess, G.D., 1998. An overview of the HYSPLIT_4 modelling system of trajectories, dispersion, and deposition. Aust. Meteor. Mag. 47, 295–308.

Wang, Y.Q., Zhang, X.Y., Draxler, R.R., 2009. TrajStat: GIS-based software that uses various trajectory statistical analysis methods to identify potential sources from long-term air pollution measurement data. Environ. Model Softw. 24 (8), 938–939. https://doi.org/10. 1016/j.envsoft.2009.01.004.

Hu, B., Zhang, X. H. and Wang, Y. S.: Variability in UVB radiation in Beijing, China, Photochem Photobiol, 89(3): 745-750, DOI: 10.1111/php.12051, 2013.

Lu, Y., Yan, C., Fu, Y., Chen, Y., Liu, Y., Yang, G., Wang, Y., Bianchi, F., Chu, B., Zhou, Y., Yin, R., Baalbaki, R., Garmash, O., Deng, C., Wang, W., Liu, Y., Petäjä, T., Kerminen, V. M., Jiang, J., Kulmala, M. and Wang, L.: A proxy for atmospheric daytime gaseous sulfuric acid concentration in urban Beijing, Atmos. Chem. Phys., 19(3): 1971-1983, DOI: 10.5194/acp-19-1971-2019, 2019.

Tang, W., Zhao, C., Geng, F., Peng, L., Zhou, G., Gao, W., Xu, J. and Tie, X.: Study of ozone “weekend effect” in Shanghai, Science in China Series D: Earth Sciences, 51(9): 1354-1360, DOI: 10.1007/s11430-008-0088-2, 2008.